Charge inversion of divalent ionic solutions in silica channels

Christian D. Lorenz and Alex Travesset
Department of Physics and Astronomy and Ames Laboratory, Iowa State University, Ames, Iowa 50011, USA
(Received 19 November 2006; revised manuscript received 21 March 2007; published 13 June 2007)

Recent experiments [F. H. J. van der Heyden *et al.*, Phys. Rev. Lett. **96**, 224502 (2006)] of streaming currents in silica nanochannels with divalent ions report charge inversion, i.e., interfacial charges attracting counterions in excess of their own nominal charge, in conflict with existing theoretical and simulation results. We reveal the mechanism of charge inversion by using all-atomic molecular dynamics simulations. Our results show excellent agreement with experiments, both qualitatively and quantitatively. We further discuss the implications of our study for the general problem of ionic correlations in solutions as well as in regards to the properties of silica-water interfaces.

DOI: 10.1103/PhysRevE.75.061202 PACS number(s): 61.20.Qg, 82.45.Mp, 82.39.Wj

I. INTRODUCTION

Counterions in aqueous solution play a crucial role in the self-assembly of colloids and polymers, cell signaling, microfluidics, and fuel cells. In recent years, there has been a considerable body of experimental and theoretical work aimed at understanding the rich and complex phenomenology of ions in aqueous solution and their interactions with charged interfaces [1–4]. A representative example of this phenomenology is charge inversion (CI), where interfacial charges attract counterions in excess of their own nominal charge, thus leading to an interface whose effective surface charge is reversed. The first simulation study that showed evidence of CI with divalent ions was conducted by Torrie and Valleau [5], in which the authors used a primitive hard sphere model for the ions and a continuum solvent model with a dielectric constant. Still the origins of CI are poorly understood, as highlighted in a recent review paper by Lyklema [6]. In particular, it is unclear to what extent existing theories explain the observed CI reported in experimental work.

A recent experiment has provided a detailed investigation of CI by multivalent counterions from an analysis of streaming currents, the electric currents resulting from applying a pressure gradient along a charged nanofluidic channel containing electrolyte solutions (see Fig. 1) [7]. The precision and accuracy of such experiments provide a perfect arena to test existing theoretical models of CI in particular and the more general problem of ion distributions.

Different theories for CI have been proposed over the years. In Ref. [8] it was proposed that CI arises from the gain in correlation energy brought about by lateral correlations (LC) among mobile counterions. For divalent ions in silica nanochannels, this theory would predict CI at $c_{\mathrm{inv}} \sim 10$ mM [37], an order of magnitude lower than what is observed experimentally [7]. In Refs. [9,10] it has been pointed out that the intrinsic discreteness of interfacial charges may give rise to CI by transverse correlations (TC), that is, correlations between counterions and interfacial charges. In particular, it has been shown that binding constants of divalent ions to oxygen atoms are typically of the order of $K_B \sim 10\ \mathrm{M}^{-1}$, thus implying CI at $c_{\mathrm{inv}} \sim 1/K_B \approx 0.1$ M. Numerical simulations with primitive models, where the solvent is considered implicitly as a medium of dielectric constant ε, have been reported [11–13], and show general agreement with LC theories, thus implying lower than the $c_{\mathrm{inv}} \approx 400$ mM observed in experiments [7]. Other theoretical work has focused on the computation of mobilities [14] as a function of ζ-potential, but as reviewed in [6], the interpretation of experimentally determined ζ-potentials is not entirely clear. A clear understanding of the CI phenomenon may therefore require approaches where water is considered explicitly and the interface is modeled realistically, with more structure than a uniform surface charge. As discussed in [10,15], these effects are expected to play a critical role.

In this paper, we investigate the origin of CI with atomic resolution by using molecular dynamics (MD) simulations of a charged silica interface in contact with an aqueous solution with divalent ions. This study is further motivated by recent interest in understanding the structure of pure water in contact with silica [16–20], as some evidence suggests the presence of highly ordered interfacial water structures. It has not been investigated, however, how divalent ions, which have a very cohesive hydration sheath, may modify interfacial wa-

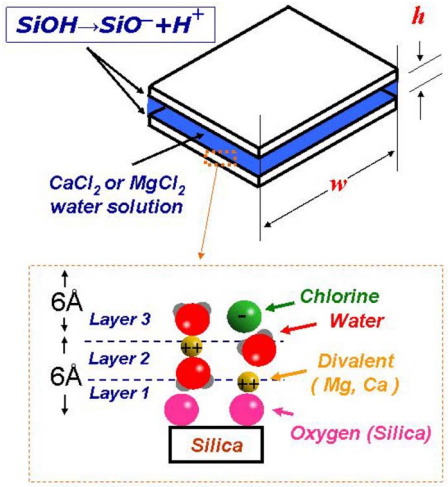

FIG. 1. (Color online) Diagram showing a silica nanochannel. Very near to the silica interface, we identify a first layer of bound counterions (layer 1), a layer of hydrated counterions (layer 2), and a third layer (layer 3), which corresponds to the diffuse layer and exhibits CI.

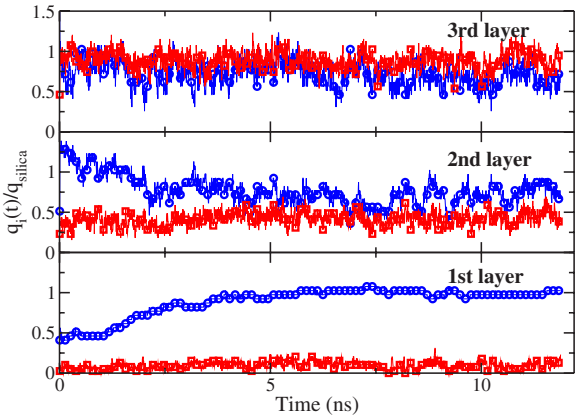

FIG. 2. (Color online) Evolution of the Ca^{2+} charge (blue circle) and Cl^- charge (red square) relative to the interfacial charge as a function of time for the different layers. Layer 1 represents bound oxygens (defined such that O-Ca^{2+} distance is less than 3 Å), layer 2 is defined by the size of the hydrated divalent ions (O-Ca^{2+} distance is within 3 and 6 Å), and layer 3 is the last layer before bulk values are attained, with O-Ca^{2+} distance <12 Å. (See Fig. 1 for a schematic definition of the different layers) Results are for 1.0 M concentrations.

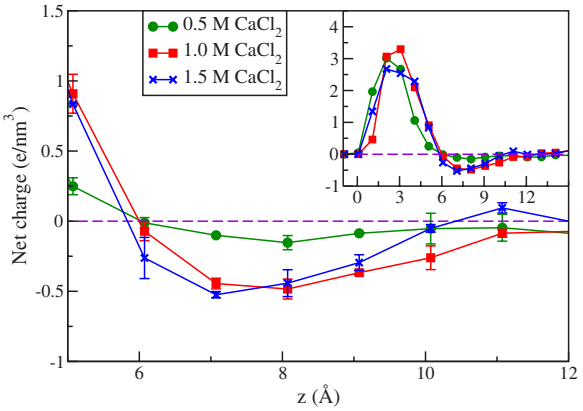

FIG. 3. (Color online) Net charge density on the third layer (see Fig. 1 for a definition of the layers) for different concentrations of $CaCl_2$. The inset shows the profile of the charge density.

ter. In addition, our results have implications in the field of microfluidics because silica is the most common material used in nanofluidic and microfluidic devices [21], including the recently synthesized nanoporous functionalized silica thin films [22,23] that are being investigated as desalination membranes [24].

II. SIMULATION DETAILS

We consider the system schematically shown in Fig. 1 where an interface of amorphous silica is in contact with an aqueous solution. Throughout this paper, we will consider ionic strengths such that $\lambda_D << h$, where λ_D is the Debye length and h is the separation between the two silica interfaces (see Fig. 1). We can therefore neglect the interactions between the two silica interfaces and perform our MD simulations on a single interface.

Amorphous silica was generated according to a previously reported procedure [25,26]. We start with a bulk α-quartz crystalline substrate that is heated to high temperature (~2500 K) and quenched to 300 K. We then generate two free surfaces in the z dimension and further anneal the substrate until the density of bond defects on each interface is representative of the experimentally observed density on amorphous silica ($4.0-5.0/nm^2$) [27]. The silicon and oxygen defects are terminated with −OH and −H, respectively. The silica interface is given a negative charge by randomly selecting −OH groups and removing the corresponding proton, leaving a net surface charge of $\sim 1e/110$ Å^{-2}, in line with experimental results [7]. The amorphous silica had a total area of 68.7076×68.082 Å^2 in contact with an aqueous solution containing water (~8500 water molecules) and divalent ions. Water was modeled explicitly by using the TIP3P model [28], the two cations used in the simulation (Ca^{2+}, Mg^{2+}), were modeled with Aqvist's parameters [29] and Cl^- with the OPLS force field [30]. The silica was modeled by the OPLS force field described in [31].

The simulations reported in this paper were performed with the LAMMPS molecular dynamics code [32]. In all simulations, the temperature is fixed at $T \approx 300$ K and controlled with a Nose-Hoover thermostat and a time constant of 0.01 fs^{-1}. The SHAKE algorithm [33] was used to constrain the bond lengths and angles of the water molecule and the bond lengths of the OH bonds on the silica substrate surface. A 1 fs time step was used and the van der Waals (vdW) interaction is cut off at 10 Å. A slab version of the particle-particle particle-mesh algorithm [34] is used to compute long-range Coulombic interactions. An average run lasted around 12 ns, with data being collected and analyzed over the last 8 ns. A typical run took 4608 node hours per 12 ns simulation.

III. SIMULATION RESULTS

It is convenient to divide the region near the silica interface into three layers as depicted in Fig. 1. The first layer is defined so that it includes all partially dehydrated divalent ions bound to silica oxygens. The second layer includes all counterions within a distance of 6 Å (measured from the center of the silica oxygens) and basically consists of hydrated counterions. The third layer extends up to a region of 12 Å, beyond which bulk density profiles are attained. We recall that in textbooks in physical chemistry [35], layer 1 is referred to as the inner Helmholtz plane, layer 2 as the outer Helmholtz plane, and layer 3 as the diffuse layer. The time evolution for the population of both Ca^{2+} and Cl^- on the different layers are shown in Fig. 2 at 1.0 M concentration. The population is expressed as a function of total charge of the ionic species within the layer relative to the total net interfacial charge. As is clear from Fig. 2, the population of the different layers reaches equilibrium after an initial period of about 3 ns. We further measured residence times and found that the average residence time for Ca^{2+} ions were ~2.0 ns, ~200 ps, and ~30 ps in the first, second, and third layers, respectively. The total simulation time for our simulations was 12 ns thus providing ample time to compute

TABLE I. Relative charge population of the ionic species of Ca^{2+} and Cl^- in each layer. Values in parentheses represent fluctuations in the last digit(s).

	First layer		Second layer		Third layer	
System	Ca^{2+}	Cl^-	Ca^{2+}	Cl^-	Ca^{2+}	Cl^-
0.5 M	0.68(41)	0.02(1)	0.54(23)	0.13(2)	0.33(7)	0.36(8)
1.0 M	0.99(29)	0.10(2)	0.69(13)	0.43(6)	0.70(18)	0.88(12)
1.5 M	0.92(40)	0.11(1)	0.85(27)	0.55(19)	1.03(26)	1.14(17)

equilibrium quantities. No significant differences were observed for other $CaCl_2$ concentrations. A summary of the average populations within different layers is shown in Table I.

Results for $MgCl_2$, however, show significant differences, as residence times in the first and second layer are surprisingly long. As an example, within 12 ns, only a single Mg^{2+} ion was exchanged from the first to the second layer. It is therefore possible that the first and second layer for $MgCl_2$ are not thermalized. The results for the $MgCl_2$ solutions are also of interest as will be clear, so in view of these caveats we will relegate a detailed summary of these results to the Appendix.

The analysis of the time series Fig. 2 and Table I shows that the third layer has a net negative charge, that is, there is an excess of Cl^- charge over divalent charge, which is the signature of CI. This is clear from Fig. 3, where the charge density as a function of distance from the interface is shown. The results exhibit no CI at 0.2 M (not shown) and marginal CI for 0.5 M $CaCl_2$, with CI considerably amplified at larger concentrations. These results show conclusive evidence for a Stern layer consisting of divalent ions (first and second layers) followed by an "inverted" (negatively charged) diffuse layer. In all cases, charge densities reach bulk values (within the accuracy of our simulations) at 12 Å from the interface.

The structure of the ions near the silica interface is analyzed using radial distribution functions (rdfs), shown in Fig. 4 for 1.0 M solutions. The rdf corresponding to divalent ions with deprotonated silica oxygens (O_{bare}) show sharp peaks at a distance roughly equivalent to the sum of the crystallographic radius of oxygen and divalent ions providing clear evidence for binding of partially dehydrated counterions to oxygens. The inset of Fig. 4 shows a much stronger binding for Ca^{2+} ions, sufficient to virtually neutralize the interfacial charge, as is clear from Table I. The rdf also shows a maxima roughly corresponding to the sum of the radii of the hydrated divalent ion and an oxygen. Although not bound, hydrated ions are strongly correlated with silica oxygens, an effect that becomes more dramatic with Mg^{2+} ions.

We further investigated the structure and orientation of water near the interface and its relation to the observed ion distributions. A detailed study of pure water near amorphous silica interfaces will be reported elsewhere [36], here we just briefly discuss the most salient aspects related to ion distributions. It is found that the average lateral separation of water molecules near charged silica are identical with pure water results, but average distances between the water molecules and oxygens on the silica interface are significantly altered (4.0 Å as opposed to 3.2 Å for neutral silica), which we interpret as being related to the Ca^{2+} hydration sheaths pushing away other water molecules. Our MD simulations do not show evidence for any effect on the counterions attributable to a preexisting interfacial water ordering.

We briefly discuss the properties of the bulk solution as the concentrations discussed in this paper cannot be considered as dilute, and activity coefficients deviate considerably from unity. It is found that the bulk rdf of Ca^{2+}-Cl^- ions shows strong correlations with a significant peak at a dis-

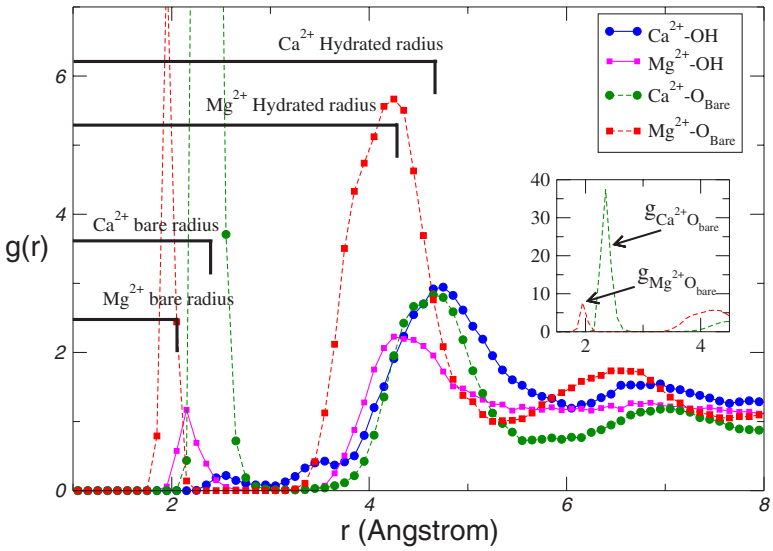

FIG. 4. (Color online) Radials distribution function of deprotonated silica oxygen atoms (O_{bare}) and protonated oxygen atoms (OH) with Ca^{2+}. The inset shows the rdf for (O_{bare})-divalent ions at a larger vertical scale.

tance corresponding to the sum of the crystallographic radius of both ions (results not shown), thus providing clear evidence for Bjerrum pairing. A quantitative analysis shows that the bulk solutions contain 8(2)%, 17(5)%, and 25(7)% of Bjerrum pairs for concentrations of 0.5 M, 1.0 M, and 1.5 M, respectively.

IV. DISCUSSION AND CONCLUSIONS

We now estimate the magnitude of the streaming current that would be measured in the systems investigated. We consider a channel with length L, width w, and height h (see Fig. 1). The streaming current is

$$I_{\mathrm{str}} = w \int_{-h/2}^{h/2} dz \rho_c(z) v(z), \tag{1}$$

where $\rho_c(z)$ is the net charge at position z and $v(z)$ is the velocity of the fluid along the channel. This velocity is given by Poiseuille flow $v(z) = \frac{\Delta P}{2\eta L}\left[z^2 - \left(\frac{h}{2}\right)^2\right]$, where $\eta \sim 0.9$ cP is the shear viscosity of water. Using the values of $\rho_c(z)$ from our simulation, explicit values for the streaming current are obtained. For wide silica channels ($h \gg \lambda_D$), this expression is further related to the ζ-potential,

$$I_{\mathrm{str}} = 2w \frac{\Delta P h}{2\eta L} \int_0^{\infty} dz z \rho_c(z) = -\Delta P \frac{wh\varepsilon_r}{4\pi\eta L}\zeta, \tag{2}$$

where $\rho_c(z)$ is the net charge distribution on an infinite slab and $\varepsilon_r \sim 80$ is the dielectric constant of water. The value of the ζ-potential is defined at the plane where the fluid velocity is zero, which we assume coincides with the boundary between the Stern and the diffuse layer [6]. Using $h=140$ nm, $w=50$ μm, and a length of the channel $L=4.5$ mm as typical values [7], we obtain $I_{\mathrm{str}} \approx 1$ pA/bar ($\zeta \approx 30$ mV) at concentrations of 1 and 1.5 M (at 0.5 M, $0 < I_{\mathrm{str}} < 0.3$ pA/bar).

This paper has presented all-atomic MD simulations of divalent ionic solutions in silica channels. Our simulations show no CI at 0.2 M so $0.2 < c_{\mathrm{inv}} < 0.5$ M. At concentrations larger than 0.5 M, CI is substantial, both for $CaCl_2$ and $MgCl_2$. At concentrations of 1.0 M, we calculate a streaming current of the order of 1 pA/bar. These results compare extremely well with the experiments in Ref. [7].

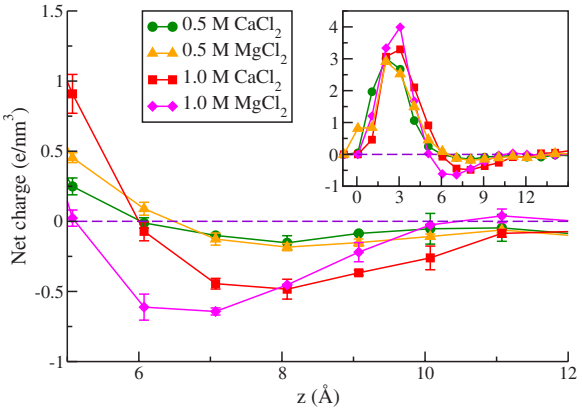

FIG. 5. (Color online) Net charge density on the third layer (see Fig. 1 for a definition of the layers) for different concentrations of $MgCl_2$ and $CaCl_2$. The inset shows the profile of the charge density.

Our simulations provide a detailed understanding of the structure of the ions near the interface and the underlying mechanism for CI. It is shown that the Stern layer consists of both bound, partially dehydrated (layer 1 or inner Helmholtz plane), and mobile hydrated counterions (layer 2 or outer Helmholtz plane). Counterions in layer 2 are strongly localized near the silica oxygens. In $CaCl_2$ solutions, the population of the inner Helmholtz plane is significantly larger than the outer plane. Overall, our results support a picture where CI is due to electrostatic correlations between counterions and discrete interfacial groups (TC) or Bjerrum pairing [9]. This is particularly clear in ions with softer hydration sheaths, such as Ca^{2+}.

In summary, in this paper we provided a detailed account of the mechanism of CI of divalent aqueous solutions near silica, in excellent agreement with experimental results [7]. By conducting simulations in which the water is explicitly modeled and the silica substrate is modeled in a realistic manner with discrete charges, we are able to capture the atomistic physics (i.e., structure of the ions and water near the charged species on the silica substrate) that plays such a large role in interfacial phenomena like that present in this problem. It remains as a future challenge to develop simpler analytical models and further quantitative experimental tests.

ACKNOWLEDGMENTS

One of the authors (A.T.) thanks S. Lemay for inspiring discussions and R. Biswas for insightful remarks on silica. One of the authors (C.L.) acknowledges discussions with E. B. Webb III, M. Stevens, G. S. Grest, M. Chandross, and M. Tsige. The authors thank J. Anderson, J. Faraudo, and D. Vaknin for valuable discussions. One of the authors (A.T.) acknowledges the Aspen Center for Physics for hospitality. This work was supported by NSF Grant No. DMR-0426597 and partially supported by DOE through the Ames Laboratory under Contract No. W-7405-Eng-82.

APPENDIX

Table II shows the average populations of the Mg^{2+} and Cl^- ions in the three layers as defined in Fig. 1. The values in Table II show that the first two layers have a net positive charge, and the third layer has a net negative charge. This behavior is a signature of charge inversion and it is the same general behavior that was observed in the $CaCl_2$ systems. The difference between the two systems is that in the $MgCl_2$ systems the silica charge is compensated by Mg^{2+} in the second layer, whereas in the $CaCl_2$ systems the silica charge is compensated by Ca^{2+} in the first layer.

Charge inversion in the $MgCl_2$ systems is also obvious in Fig. 5, where the charge density as a function of distance from the interface is shown. The data from the $CaCl_2$ systems are also plotted in Fig. 5 so that they can be compared to the $MgCl_2$ systems. In both cases, there is marginal CI of nearly identical magnitude at a concentration of 0.5 M. Then

TABLE II. Relative charge population of the ionic species of Mg^{2+} and Cl^- in each layer. Values in parentheses represent fluctuations in the last digit(s).

	First layer		Second layer		Third layer	
System	Mg^{2+}	Cl^-	Mg^{2+}	Cl^-	Mg^{2+}	Cl^-
0.5 M	0.26	0.03(1)	0.99(20)	0.14(2)	0.32(6)	0.38(8)
1.0 M	0.15	0.08(1)	1.54(39)	0.43(11)	0.65(8)	0.84(13)

at a concentration of 1.0 M, both systems show significantly larger CI. These results for the $MgCl_2$ systems show conclusive evidence for a Stern layer consisting of Mg^{2+} ions (first and second layers) followed by an "inverted" (negatively charged) diffuse layer.

In $MgCl_2$ solutions, the number of divalent ions within the Stern layer is similar as in $CaCl_2$ but its structure is quite different, as there are very few bound counterions. We raised the possibility that this may reflect that the Stern layer may not be thermalized, and that longer simulations (at least $\sim 1\ \mu s$) might reveal a structure more similar to the $CaCl_2$ case. We point out, however, that in Ref. [9] it was concluded that binding constants of Mg^{2+} to oxygen atoms are generally small, a result attributed to the compactness of the Mg^{2+} hydration sheath. In any case, whether thermalized or not, our simulations show CI and, as apparent from the rdf in Fig. 4, correlations between Mg^{2+} and charged interfacial groups are shown to play a fundamental role.

[1] S. McLaughlin, Annu. Rev. Biophys. Biophys. Chem. **18**, 113 (1989).
[2] A. Yu. Grosberg, T. T. Nguyen, and B. I. Shklovskii, Rev. Mod. Phys. **74**, 329 (2002).
[3] Y. Levin, Rep. Prog. Phys. **65**, 1577 (2002).
[4] H. Boroudjerdi *et al.*, Phys. Rep. **416**, 129 (2005).
[5] G. M. Torrie and J. P. Valleau, J. Phys. Chem. **86**, 3251 (1982).
[6] J. Lyklema, Colloids Surf., A **291**, 3 (2006).
[7] F. H. J. van der Heyden, D. Stein, K. Besteman, S. G. Lemay, and C. Dekker, Phys. Rev. Lett. **96**, 224502 (2006).
[8] B. I. Shklovskii, Phys. Rev. E **60**, 5802 (1999).
[9] A. Travesset and D. Vaknin, Europhys. Lett. **74**, 181 (2006).
[10] J. Faraudo and A. Travesset, J. Phys. Chem. C **111**, 987 (2006).
[11] M. Trulsson, B. Jonsson, T. Akesson, J. Forsman, and C. Labbez, Phys. Rev. Lett. **97**, 068302 (2006).
[12] A. Diehl and Y. Levin, J. Chem. Phys. **125**, 054902 (2006).
[13] A. Martin-Molina *et al.*, J. Chem. Phys. **125**, 144906 (2006).
[14] M. Lozada-Cassou and E. Gonzalez-Tovar, J. Colloid Interface Sci. **239**, 285 (2001).
[15] J. Faraudo and F. Bresme, Phys. Rev. Lett. **92**, 236102 (2004).
[16] S. Engemann, H. Reichert, H. Dosch, J. Bilgram, V. Honkimaki, and A. Snigirev, Phys. Rev. Lett. **92**, 205701 (2004).
[17] V. Ostroverkhov, G. A. Waychunas, and Y. R. Shen, Phys. Rev. Lett. **94**, 046102 (2005).
[18] I. M. P. Aarts, A. C. R. Pipino, J. P. M. Hoefnagels, W. M. M. Kessels, and M. C. M. Van de Sanden, Phys. Rev. Lett. **95**, 166104 (2005).
[19] D. B. Asay and S. H. Kim, J. Phys. Chem. B **109**, 16760 (2005).
[20] S. Joseph and N. R. Aluru, Langmuir **22**, 9041 (2006).
[21] H. A. Stone, A. D. Stroock, and A. Ajdari, Annu. Rev. Fluid Mech. **36**, 381 (2004).
[22] D. A. Doshi *et al.*, Science **290**, 107 (2000).
[23] N. G. Liu, R. A. Assink, and C. J. Brinker, Chem. Commun. (Cambridge) **3**, 370 (2003).
[24] K. Leung, S. B. Rempe, and C. D. Lorenz, Phys. Rev. Lett. **96**, 095504 (2006).
[25] M. Chandross, E. B. Webb III, M. J. Stevens, G. S. Grest, and S. H. Garofalini, Phys. Rev. Lett. **93**, 166103 (2004).
[26] C. D. Lorenz *et al.*, Tribol. Lett. **19**, 93 (2005).
[27] L. T. Zhuravlev, Colloids Surf., A **173**, 1 (2000).
[28] W. L. Jorgensen *et al.*, J. Chem. Phys. **79**, 926 (1983).
[29] J. Aqvist, J. Phys. Chem. **94**, 8021 (1990).
[30] J. Chandrasekhar, D. Spellmeyer, and W. L. Jorgensen, J. Am. Chem. Soc. **106**, 903 (1984).
[31] W. L. Jorgensen, D. S. Maxwell, and J. Tirado-Rives, J. Am. Chem. Soc. **118**, 11225 (1996); W. L. Jorgensen (private communication).
[32] S. J. Plimpton, J. Comput. Phys. **117**, 1 (1995).
[33] J. P. Ryckaert, G. Ciccotti, and H. J. C. Berendsen, J. Comput. Phys. **23**, 327 (1977).
[34] P. S. Crozier, R. L. Rowley, and D. Henderson, J. Chem. Phys. **114**, 7513 (2001).
[35] J. Lyklema, *Fundamentals of Interface and Colloid Science*, (Academic, San Diego, 1995).
[36] C. D. Lorenz *et al.* (unpublished).
[37] The plasma parameter Γ may be too small for this theory to rigorously apply [2].